AC-driven Quantum Phase Transition in the Lipkin-Meshkov-Glick Model

G. Engelhardt,* V. M. Bastidas,† C. Emary, and T. Brandes
Institut für Theoretische Physik, Technische Universität Berlin, Hardenbergstr. 36, 10623 Berlin, Germany

We establish a set of nonequilibrium quantum phase transitions in the Lipkin-Meshkov-Glick model driven under monochromatic nonadiabatic modulation of the transverse field. We show that the external driving induces a rich phase diagram that characterizes the multistability in the system. Interestingly, the number of stable configurations can be tuned by increasing the amplitude of the driving field. Furthermore, by studying the quantum evolution , we demonstrate that the system exhibits a set of quantum phases that correspond to dynamically stabilized states.

PACS numbers: 32.80.Qk, 21.60.Ev, 05.30.Rt, 03.75.Kk

A quantum phase transition (QPT) is a drastic change of state of a many-body system which occurs at zero temperature [1]. In contrast to thermodynamic phase transitions—which are driven by thermal fluctuations, QPTs are entirely driven by quantum fluctuations. This critical behavior gives rise to states of matter, which—in some cases, can be described in terms of symmetry-broken phases. Most of the research in the past has been focused on QPTs on equilibrium systems, whereas relatively little is known about the critical behavior in nonequilibrium conditions. The quantum control of many-body systems by a driving field has attracted considerable interest both theoretical and experimental with workers from very different communities beginning to look at driven models [2–12]. The possibility to manipulate the quantum state of a system by means of a classical external control allows one to explore novel states of matter and effective interactions which are absent in equilibrium [11–14]. In this context, a recent line of research are excited-state phase transitions, e.g. in mean-field type QPTs such as the Lipkin-Meshkov-Glick [15] or the Dicke superradiance [16] model. Furthermore, the connection between chaos and criticality [17] has been studied in detail for the interacting boson model [18].

Despite of the original motivation of the Lipkin-Meshkov-Glick (LMG) model as a toy model to test approximation methods in manybody physics [19], currently it constitutes an active field of research and a natural scenario to study the relation between QPTs and spin squeezing [20] and quantum Fisher information as a resource for high-precision quantum estimation [21]. Furthermore, rather recently, experimental realizations of the LMG model in optical cavity QED [22, 23] and circuit QED [24] have been suggested.

In this paper we study a driven version of the LMG model in which we assume a time-dependent interparticle interaction. In comparison with previous works which considered dynamical properties of the LMG model under an adiabatic change of parameters of the system across the quantum critical point [25], the effect of fast and slow quenches of the transverse field [26], and a periodically-driven uniaxial LMG model [6, 27, 28], we address here the fundamental issue of driving-induced QPTs in the LMG model.

The development of novel experimental techniques to externally control many-body systems has been extensively increased in the last years. For example, the kicked top, has been realised experimentally in an ensemble of laser-cooled Cs atoms [29]. Furthermore, an optical realization of the uniaxial driven LMG in photonic lattices [30] and by using superconducting charge qubits connected in parallel to a common superconductor inductance [31] have been suggested.

We show that when the driving is near resonance with the excitation energy of the undriven system the nature of criticality changes dramatically. Additionally, we find a phase diagram replete with a host of macroscopically distinct metastable phases with no analogues in equilibrium. This gives rise to a novel route of experimental studies exploring the characteristics of criticality under nonequilibrium conditions.

A more specific outline of our paper is as follows. In section I we describe the fundamentals on the QPT in the undriven LMG model and construct a bosonized effective Hamiltonian which allows us to describe the stability properties of the symmetric phase. In section II we find an effective Hamiltonian by using the rotating wave approximation (RWA) and describe the quantum evolution of the observables to understand the characteristics of the novel nonequilibrium metastable phases. Finally, conclusive remarks are given in section III.

I. QUANTUM RESONANCES IN THE LMG MODEL.

The periodically-driven Lipkin-Meshkov-Glick model describes the dynamics of N interacting two-level systems in a transverse local field

$$\hat{H}(t) = -hJ_z - \frac{1}{N}\left(\gamma^x(t){J_x}^2 + \gamma^y {J_y}^2\right), \qquad (1)$$

where $J_\alpha = \frac{1}{2}\sum_{i=1}^{N}\sigma_\alpha^{(i)}$ denote collective angular momentum operators and $\sigma_\alpha^{(i)}$ are the Pauli matrices with

*Electronic address: georgt@itp.tu-berlin.de
†Electronic address: victor@physik.tu-berlin.de

$\alpha \in \{x, y, z\}$. These operators satisfy the $SU(2)$ algebra $[J_\alpha, J_\beta] = i\epsilon_{\alpha\beta\gamma}J_\gamma$. In the following we shall consider $h < 0$, and a monochromatic modulation of the interparticle interaction with a static contribution: $\gamma^x(t) = \gamma_0^x + \gamma_1^x \cos\Omega t$.
In this paper we consider Dicke states i.e., the whole analysis is reduced to the Hilbert subspace characterized by a maximal total angular momentum $j = N/2$. Associated with the Hamiltonian Eq. (1) is a conserved parity

$$\hat{\Pi} = \exp(i\pi(J_z + j)), \tag{2}$$

such that $[\hat{H}(t), \hat{\Pi}] = 0$. Our aim in this paper is to study the new aspects of criticality under the effect of driving. In this section we provide the basics on the formalism used to describe the effective Hamiltonian for the symmetric phase of the LMG model. In particular, we find a resonance condition related to m-photon processes under the effect of driving.

A. The QPT in the undriven LMG model

In the case of the undriven LMG model ($\gamma_1^x = 0$), an analytic study of the ground-state energy surface in the thermodynamic limit $N \to \infty$ leads to a phase diagram in the (γ_0^x, γ^y)-plane, which is divided into four regions depending on the geometry of the surface. These sections are distinguished from each other by the number of minima, maxima and saddle points, which are related to non-analyticities of the density of states [15]. As a consequence of the symmetry of the LMG Hamiltonian, it is sufficient to consider the region with $|\gamma_0^x| < \gamma^y$. This analysis shows that in region $|\gamma_0^x| < \gamma^y < -h$ the ground-state energy landscape has a single global minimum, whereas in the regions with $|\gamma_0^x| < -h < \gamma^y$ the surface has two global minima. By crossing the critical line $\gamma^y = -h$, the single global minimum splits in two global minima and the system exhibits a continous transition from a symmetric state to a symmetry-broken state, i.e., a second-order QPT.

B. Effective bosonized Hamiltonian for the symmetric phase

We begin our analysis by investigating the stability of the symmetric phase under the effect of an external driving. To this end, we construct a symmetric phase effective Hamiltonian in the same way as in Ref. [13]: we make a Holstein-Primakoff representation of the angular momentum algebra in terms of bosonic operators $b, b^\dagger$

$$\begin{aligned} J_z &= b^\dagger b - \frac{N}{2}, \\ J_+ &= b^\dagger \sqrt{N - b^\dagger b}, \\ J_- &= \sqrt{N - b^\dagger b}\ b, \end{aligned} \tag{3}$$

and take the thermodynamic limit $N \to \infty$, assuming $b/N \to 0$. The result is a bosonized Hamiltonian for the symmetric phase

$$\hat{H}_S(t) = -h\, b^\dagger b - \frac{1}{4}[\gamma^x(t)(b^\dagger + b)^2 - \gamma^y(b^\dagger - b)^2] + \frac{Nh}{2}. \tag{4}$$

By introducing the coordinate operators

$$\hat{q} = \sqrt{-\frac{1}{2h}\left(\frac{h}{h+\gamma^y}\right)}(b^\dagger + b), \tag{5}$$

$$\hat{p} = i\sqrt{-\frac{h}{2}\left(1 + \frac{\gamma^y}{h}\right)}(b^\dagger - b), \tag{6}$$

we obtain the Hamiltonian of a parametrically-driven harmonic oscillator [32]

$$\hat{H}_S(t) = \frac{\hat{p}^2}{2} + \frac{1}{2}\left(\epsilon^2 + h\gamma_1^x\left(1 + \frac{\gamma^y}{h}\right)\cos\Omega t\right)\hat{q}^2 + \frac{Nh}{2}, \tag{7}$$

where

$$\epsilon = -h\sqrt{\left(1 + \frac{\gamma^y}{h}\right)\left(1 + \frac{\gamma_0^x}{h}\right)} \tag{8}$$

is the characteristic energy scale of the system in the absence of driving ($\gamma_1^x = 0$). The undriven system exhibits a critical behavior which is related to softening of the collective excitation spectrum, i.e., when the system is close to the critical point ($\gamma^y \to -h$), the system exhibits a gapless excitation above the ground state ($\epsilon \to 0$). Therefore, in the region $|\gamma_0^x| < -h < \gamma^y$ the symmetric phase became unstable. Interestingly, in the driven system the situation can be highly nontrivial as a consequence of mechanisms such as parametric resonance and parametric stabilization, which are characteristic of the parametrically-driven harmonic oscillator [13, 32]. As a consequence, one can tune up conveniently the parameters close to resonance in order to manipulate the stability of the system, i.e., to produce a change of phase for parameters which are far away from the critical point of the undriven system.

C. Resonance conditions

In the thermodynamic limit, the undriven LMG model is characterized by a single collective excitation with energy ϵ. Under the effect of an external driving, the possibility of multiphotonic resonances arises [33–35]. In the semiclassical theory of light-matter interaction, we can interpret a Floquet state as a light-matter quantum state containing a definite, though very large, number of photons [33]. Multiple transitions between quantum states of system that are not directly coupled by the interaction can occur by means of intermediate states with a different number of photons present [33, 34, 36]. In particular, m-photon transitions occur when the condition

$$2\epsilon = m\Omega, \tag{9}$$

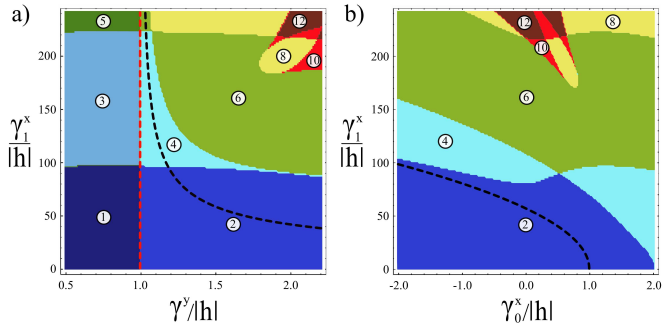

FIG. 1: (Color online) Phase diagram of the nonequilibrium QPT in the Lipkin-Meshkov-Glick model. The number of local minima of the quasienergy surface $E_G^{(0)}(Q,P)$ in the colored zones are indicated by the labels. (a) Depicts the phase diagram as a function of γ^y and the driving amplitude γ_1^x for $\gamma_0^x/|h| = 0.5$, and (b) as a function of γ_0^x and γ_1^x for $\gamma^y/|h| = 2$. The dashed red (light gray) line in (a) resembles the second-order QPT in the undriven LMG model that occurs at $\gamma^y/|h| = 1$, in the driven case, however, this line is the separatrix between the regions with even and odd number of minima. The dashed black lines in (a) and (b) depict the transition of the symmetric phase $(Q,P) = (0,0)$ from a saddle point to a local maximum, and correspond to the contour $\lambda_2 = 0$. We consider the parameters $\Omega/|h| = 40$ and $h/|h| = -1$.

with integer m is satisfied. For a parametric oscillator with fundamental frequency ϵ, Eq. (9) is the usual resonance condition [32]. In Floquet theory, Eq. (9) implies the existence of a crossing between the energy levels when the energy spectrum of the undriven system is folded into the Brillouin zone [33]. In this paper we focus on the parameter regime $\delta^{(m)}, \gamma_0^x, \gamma^y \ll \Omega$, where the detuning $\delta^{(m)} = -h - \frac{m\Omega}{2}$ describes how far the system is from resonance, and the resonance condition Eq. (9) reads

$$-h \approx \frac{m\Omega}{2}. \tag{10}$$

Such resonance condition will be used in the next section to perform a description of the system based on an effective time-independent Hamiltonian which is valid for parameters close to a multiphotonic resonance.

II. THE ROTATING WAVE APPROXIMATION AND THE EFFECTIVE HAMILTONIAN APPROACH

As we are interested in the asymptotic quantum dynamics and the description of critical signatures, it is convenient to describe the dynamics of the system in a rotating frame. In the limit $\delta^{(m)}, \gamma_0^x, \gamma^y \ll \Omega$, it is possible to neglect the fast oscillations in the rotating frame, and a treatment of the system based on the description for time-independent systems is possible via an approximate effective Hamiltonian. Motivated by the m-photon resonance condition Eq. (10), we perform a study of the system based on the rotating wave approximation (RWA) [13, 36]. Let us perform an unitary transformation of Hamiltonian Eq. (1) into a convenient rotating frame via the unitary operator

$$\hat{U}_m(t) = \exp\left(-i\Theta(t)J_x^2\right)\exp\left(-i\theta_m(t)J_z\right), \tag{11}$$

where $\Theta(t) = \frac{\gamma_1^x \sin\Omega t}{N\Omega}$ and $\theta_m(t) = \frac{m\Omega t}{2}$. In the rotating frame the dynamics is governed by the Hamiltonian $\hat{H}_m(t) = \hat{U}_m^\dagger(t)\hat{\mathcal{H}}\hat{U}_m(t)$, where $\hat{\mathcal{H}} = \hat{H}(t) - i\frac{\partial}{\partial t}$ is the Floquet Hamiltonian [33]. The explicit form of this operator is given by

$$\begin{aligned}\hat{H}_m(t) &= -\frac{h}{2}[(J_z + i\hat{\Lambda}_1^m(t))\hat{\mathcal{O}}_1^m(t) + h.c] - \frac{m\Omega}{2}J_z \\ &+\frac{\gamma^y}{4N}[(J_z + i\hat{\Lambda}_1^m(t))^2\hat{\mathcal{O}}_2^m(t) + h.c] \\ &-\frac{\gamma^y}{2N}[J_z^2 + (\hat{\Lambda}_1^m(t))^2] - \frac{\gamma_0^x}{N}(\hat{\Lambda}_2^m(t))^2.\end{aligned} \tag{12}$$

We consider here the notation

$$\hat{\mathcal{O}}_1^m(t) = \sum_{l=-\infty}^{\infty}\mathcal{J}_l\left[\frac{\gamma_1^x}{N\Omega}(2\hat{\Lambda}_2^m(t)+1)\right]e^{il\Omega t}, \tag{13}$$

$$\hat{\mathcal{O}}_2^m(t) = \sum_{l=-\infty}^{\infty}\mathcal{J}_l\left[\frac{4\gamma_1^x}{N\Omega}(\hat{\Lambda}_2^m(t)+1)\right]e^{il\Omega t}, \tag{14}$$

where $\mathcal{J}_l(z)$ is the lth-order Bessel function [37], and

$$\hat{\Lambda}_1^m(t) = -J_y\cos\theta_m(t) - J_x\sin\theta_m(t), \tag{15}$$

$$\hat{\Lambda}_2^m(t) = J_x\cos\theta_m(t) - J_y\sin\theta_m(t). \tag{16}$$

The Hamiltonian Eq. (12) can be written in the form

$$\hat{H}_m(t) = \sum_{n=-\infty}^{\infty}\hat{h}_n^{(m)}\exp(in\Omega t). \tag{17}$$

In analogy with the standard RWA of quantum optics, we obtain an approximate Hamiltonian to describe the mth resonance by neglecting all the terms in $\hat{H}_m(t)$ with oscillatory time-dependence: $\hat{H}_m(t) \approx \hat{h}_0^{(m)}$. The effective Hamiltonian $\hat{h}_0^{(m)}$ governs the dynamics in the rotating frame.

We next perform a bosonization procedure of $\hat{h}_0^{(m)}$ via the Holstein-Primakoff representation Eq. (3). In the bosonized version, the effective Hamiltonian is written in terms of the bosonic mode b. To investigate the criticality in the system we introduce a complex macroscopic displacement of order $\sqrt{N}$ for the bosonic operator as follows

$$b = c + \alpha\sqrt{N}, \tag{18}$$

where $\alpha = (Q + iP)$ (Q and P are dimensionless parameters) and c is a bosonic operator describing quantum fluctuations in the system. In the thermodynamic limit

$N \to \infty$, we perform a series expansion of the effective Hamiltonian in powers of $\sqrt{N}$

$$\hat{h}_0^{(m)} = \hat{h}_Q^{(m)}(c, c^\dagger) + \sqrt{N}\, \hat{h}_L^{(m)}(c, c^\dagger) + N E_G^{(m)}(Q, P), \tag{19}$$

where $\hat{h}_Q^{(m)}(c, c^\dagger)$ is a quadratic bosonic Hamiltonian (depending on the choice of the macroscopic displacements Eq. (18)), $\hat{h}_L^{(m)}(c, c^\dagger)$ contains linear bosonic terms, and $E_G^{(m)}(Q, P)$ is the lowest quasienergy (LQE).

A. The effective Hamiltonian for the $m = 0$ case

Instead of performing an abstract general theory for the effective Hamiltonian related to general m-photon resonances, we focus here on an illustrative particular case that contains the more relevant information, i.e., we consider the case $m = 0$. In this case, the effective Hamiltonian reads

$$\hat{h}_0^{(0)} = \left[-\frac{h}{2}(J_z - iJ_y)\mathcal{J}_0\left[\frac{\gamma_1^x}{N\Omega}(2J_x + 1)\right] + \frac{\gamma^y}{4N}(J_z - iJ_y)^2 \mathcal{J}_0\left[\frac{4\gamma_1^x}{N\Omega}(J_x + 1)\right] + h.c\right] - \frac{\gamma^y}{2N}(J_z^2 + J_y^2) - \frac{\gamma_0^x}{N}J_x^2 \ . \tag{20}$$

In the thermodynamic limit $N \to \infty$, we expand the Holstein-Primakoff representation Eq.(3) with respect to the complex macroscopic displacement Eq. (18) up to leading order N

$$J_x = NQ\sqrt{1 - |\alpha|^2}, \tag{21}$$

$$J_y = NP\sqrt{1 - |\alpha|^2}, \tag{22}$$

$$J_z = N\left(|\alpha|^2 - \frac{1}{2}\right). \tag{23}$$

This transformation describes a mapping from the coordinates (Q, P) onto the Bloch sphere, because the norm of the spin vector (J_x, J_y, J_z) has constant length $J = N/2$. From Eqs. (21) and (22) it follows that $|\alpha|^2 \leq 1$. Furthermore, one can see from these relations that all points (Q, P) with $|\alpha|^2 = 1$ correspond to $J_z = N/2$. Therefore, all points of the boundary $|\alpha|^2 = 1$ are mapped into the north pole of the Bloch sphere. For the interior points $|\alpha|^2 < 1$, the transformation is bijective, e.g., the origin $(Q, P) = (0, 0)$ is mapped into the south pole.

By replacing Eqs. (21),(22), and (23) into the effective Hamiltonian Eq. (20) we obtain the LQE for the $m = 0$ case

$$\begin{aligned} E_G^{(0)}(Q, P) \ = \ & -h\left(|\alpha|^2 - \frac{1}{2}\right)\mathcal{J}_0\left[\frac{2\gamma_1^x}{\Omega}Q\sqrt{1 - |\alpha|^2}\right] - \frac{\gamma^y}{2}\left[\left(|\alpha|^2 - \frac{1}{2}\right)^2 + \left(1 - |\alpha|^2\right)P^2\right] \\ & + \frac{\gamma^y}{2}\left[\left(|\alpha|^2 - \frac{1}{2}\right)^2 - \left(1 - |\alpha|^2\right)P^2\right]\mathcal{J}_0\left[\frac{4\gamma_1^x}{\Omega}Q\sqrt{1 - |\alpha|^2}\right] - \gamma_0^x\left(1 - |\alpha|^2\right)Q^2. \end{aligned} \tag{24}$$

In the undriven case, a classification of the quantum phases of the LMG Hamiltonian is usually performed by studying the global minima of the energy landscape [15]. However, in this work we interpret the local minima of the LQE as metastable phases of the driven system. These metastable states are related to the phenomenon of parametric stabilization [32]. Since these are separated from the global minima by macroscopic displacements, we expect transitions to be suppressed, such that the corresponding values of the order parameters are observable. This possibility is reinforced when one recalls that $E_G^{(0)}(Q, P)$ does not have the same thermodynamic significance as the lowest actual energy. Therefore, in this work we consider the number of minima of the LQE landscape as a criterion to establish a new phase diagram.

Fig.1 (a) depicts the phase diagram as a function of γ^y and γ_1^x , for fixed $\gamma_0^x/|h| = 0.5$, and Fig.1 (b) as a function of γ_0^x and γ_1^x, for fixed $\gamma^y/|h| = 2$. In these phase diagrams, we see many regions corresponding to different number of minima of the LQE landscape. Additionally, the phase diagrams show the appearance of many novel metastable phases, which are separated from each other by boundary lines, whose crossings correspond to nonequilibrium multicritical points. By crossing the line $\gamma^y = -h$ in Fig.1, the single global minimum at $(Q, P) = (0, 0)$ splits into two macroscopically separated

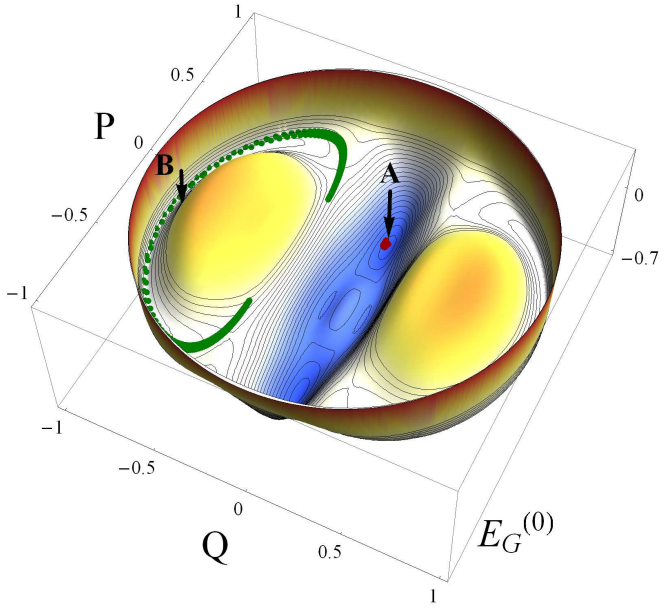

FIG. 2: Lowest quasienergy landscape for the parameters $\frac{1}{|h|}(h, \gamma_0^x, \gamma_1^x, \gamma^y) = (-1, -1, 210, 2)$. In the undriven system, these parameters correspond to the symmetry-broken phase. The quantum evolution for $N = 100$ particles within one period is calculated when the system is initialized in a spin coherent state. The green (light gray) line on the surface depicts the evolution of an initial wave packet centered at minima B and the red line shows the corresponding evolution for a wave packet initially centered at A. We consider the parameters $\Omega/|h| = 40$ and $h/|h| = -1$

.

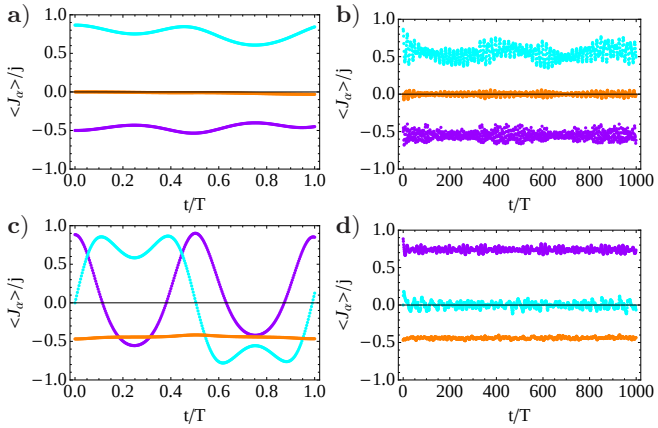

FIG. 3: Quantum evolution of the observables for finite size $N = 100$ and parameters $\frac{1}{|h|}(h, \gamma_0^x, \gamma_1^x, \gamma^y) = (-1, -1, 210, 2)$. The expectation values $\langle J_x\rangle/j, \langle J_y\rangle/j$ and $\langle J_z\rangle/j$ are depicted by the orange, cyan and magenta curves respectively. (a) Depicts the quantum evolution within one period and (b) depicts the stroboscopic dynamics when the system is initialized in a wave packet centered at the minimum A depicted in figure 2. Correspondingly, (c) and (d) depict the inter-period and stroboscopic evolution, respectively, when the system is initialized in a wave packet centered at the minimum B depicted in figure 2. We consider the parameters $\Omega/|h| = 40$, $h/|h| = -1$.

global minima thus resembling the second order QPT known from the time-independent model. Interestingly, regions with even and odd number of minima are characterized by the existence of two and one global minima respectively. We can study the stability of the global minimum at $(Q, P) = (0, 0)$ analytically by computing the Jacobian-matrix at the origin of the LQE landscape and its eigenvalues

$$\lambda_1 = -2\left(h + \gamma^y\right), \tag{25}$$

$$\lambda_2 = -2h - 2\gamma_0^x - \left(h + \gamma^y\right)\left(\frac{\gamma_1^x}{\Omega}\right)^2. \tag{26}$$

Both eigenvalues are positive in the region $\gamma_y < -h$ (the contours $\lambda_1 = 0$ and $\lambda_2 = 0$ are depicted as red (light gray) and black dashed lines respectively in Fig.1). In the region $\gamma_y > -h$ and $\gamma_1^x < \Omega\sqrt{\left(\frac{2h+2\gamma_0^x}{-h-\gamma^y}\right)}$ (region between the dashed curves in Fig.1 (a)), λ_1 is negative and λ_2 is positive. Furthermore λ_1 and λ_2 are negative for $\gamma_1^x > \Omega\sqrt{\left(\frac{2h+2\gamma_0^x}{-h-\gamma^y}\right)}$, and therefore, by crossing the curve $\lambda_2 = 0$, the saddle point at the origin becomes a local maximum. Consequently, in the region $\gamma_y > -h$ the single central minimum splits up in two global minima. The phase diagram depicted in Fig.1 (b) is characterized by $\lambda_1 < 0$, and therefore, the dashed line corresponds to the boundary between the regions below and above the level curve $\lambda_2 = 0$, where the origin is a saddle point and a maximum respectively.

An example for the LQE is given in Fig. 2, where the parameters are so chosen, that the undriven system ($\gamma_1^y = 0$) is in the symmetry-broken phase. As the LQE corresponds to the ground state energy in the undriven case, it exhibits two global minima corresponding to macroscopically separated states degenerate in energy. In the driven system, apart from the two global minima characteristic of the undriven system (in Fig. 2 denoted with A), new characteristics of the LQE landscape appear, e.g. two local minima (denoted with B). These new local minima can be interpreted to be novel metastable states, which are strongly related to the quantum evolution of the system as we describe in the next section.

B. Quantum evolution

In this section we investigate the quantum evolution when the system is initially prepared in a spin coherent state [38] centered at a local minimum of the LQE surface. Spin coherent states have minimum uncertainty and are the closest ones to a classical angular momentum state. To describe geometrically the quantum evolution, we parametrize the Bloch sphere using spherical coordi-

nates and express the angular momentum components in terms of the azimuthal (ϕ) and polar (θ) angles as follows:

$$J_x = \frac{N}{2}\sin\theta\cos\phi, \tag{27}$$

$$J_y = \frac{N}{2}\sin\theta\sin\phi, \tag{28}$$

$$J_z = -\frac{N}{2}\cos\theta. \tag{29}$$

By replacing this set of equations into Eqs. (21)-(23) we find a relation between the (θ,ϕ) and (Q,P) coordinate systems

$$\theta = \pi - \arccos\left[2\left(Q^2+P^2\right)-1\right], \tag{30}$$

$$\phi = \arccos\left[\frac{2Q}{\sin(\theta)}\sqrt{1-Q^2-P^2}\right]. \tag{31}$$

With the angular coordinates ϕ and θ, we can represent the spin coherent state $|\phi,\theta\rangle$ by using $|\phi,\theta\rangle = (1+|\tau|^2)^{-j}\exp[\tau J_+]\,|j,-j\rangle$ with $\tau = e^{-i\phi}\tan\frac{\Theta}{2}$. This procedure describes a mapping from a point of the LQE surface onto the set of spin coherent states.

To study the quantum evolution we consider a system consisting of $N = 100$ particles. For a finite size N, the numerical problem consists in the solution of $2N+1$ coupled ordinary differential equations. After the numerical integration of the Schrödinger equation, we construct the evolution operator $\hat{U}(t,0)$, which allows us to calculate the state of the system at any time $t>0$: $|\Psi,t\rangle = \hat{U}(t,0)\,|\phi,\theta\rangle$, providing that we prepare initially the system in a spin coherent state $|\Psi,0\rangle = |\phi,\theta\rangle$. We now proceed to calculate the normalized expectation values of the spin components in the state $|\Psi,t\rangle$. Fig. 3 (a) depicts the continuous time evolution within one period of the driving $T = 2\pi/\Omega$ of an initial wave packet centered at the minimum A in Fig. 2. Similarly, Fig. 3 (c) shows the inter-period dynamics when the initial wave packet is centered at the minimum B in Fig. 2. To obtain a better geometrical picture of the quantum evolution we represent the mean values of the angular momentum components by means of the coordinates Q and P. Therefore, we project the expectation values onto the Bloch sphere by calculating the angles ϕ and θ and then solving Eqs. (30) and (31) for Q and P. The result is shown in Fig. 2 for $N = 100$ particles, where the time evolution for initial wave packets centered in minima A and B is depicted by the red and green (light gray) curves, respectively. The trajectory initialized in A is strongly trapped within the minimum, whereas the other trajectory exhibits higher oscillations around the initial state. For finite size $N \gg 1$ the trajectories take place approximately over the surface of the LQE landscape, i.e., the mean value of the spin evolves in average along points with equal values of E_G^0. This behavior is connected to the fact that the eigenvalues of the effective Hamiltonian—from which the LQE is derived, correspond to the quasienergies of the system and the average value of the quasienergy is conserved in a time-periodic system. The state in the laboratory frame $|\Psi,t\rangle$ and the state in the rotating frame $|\Psi_m,t\rangle$ — in which the LQE is derived, are connected via

$$|\Psi,t\rangle = \hat{U}_m(t)|\Psi_m,t\rangle \tag{32}$$

$$\approx \hat{U}_m(t)\hat{e}^{-i\hat{h}_0^{(m)}t}|\Psi,0\rangle, \tag{33}$$

where $U_{rot}(t,0) \approx \hat{e}^{-i\hat{h}_0^{(m)}t}$ denote the propagator in the rotating frame and $|\Psi_m,0\rangle = |\Psi,0\rangle$ as a consequence of Eq. (11). Furthermore, the propagators in the laboratory and rotating frame are related as $\hat{U}(t,0) \approx \hat{U}_m(t)e^{-i\hat{h}_0^{(m)}t}$. Additionally, there is a very interesting relation between the stroboscopic quantum evolution and the parity operator Eq. (2) that can be established using the relation

$$U_m(t_r) = \left[\hat{\Pi}\exp\left(i\frac{\pi N}{2}\right)\right]^{\frac{mr}{2}}, \tag{34}$$

for $t_r = \frac{2r\pi}{\Omega}$ with integer r. As a consequence of this, for $m = 0$ we have $U_m(t_r) = I$, which implies that the states in the laboratory frame and in the rotating frame are identical for these times. Thus, the stroboscopic time evolution is governed entirely by $\hat{h}_0^{(0)}$. The stroboscopic long-time evolution of the observables is displayed in Fig. 3(b). Here, the quantum evolution is strongly trapped in the neighborhood of the minimum A in Fig. 2. A similar situation occurs in Fig. 3(d) for a wave packet initially centered at the minimum B in Fig. 2. By calculating the quantum evolution with different system sizes, one finds that the quantum fluctuations of the trajectories decrease with number of particles, and therefore, in the thermodynamic limit, the time evolution has to be constrained to the LQE landscape. Because the time evolution is connected with the geometrical features of the LQE landscape, it is justified to use it as a background to define the existence of new metastable phases.

III. CONCLUSIONS

We have investigated the driving-induced QPT in the LMG model. We show that under the effect of an external driving the system exhibits a multistable character with no analogue in equilibrium systems. In particular, the novel quantum phases correspond to local minima of the LQE landscape. To understand the nature of the nonequilibrium metastable states, we study the quantum evolution for finite size N when the system is initially prepared in a coherent state centered at one particular local minimum of the LQE surface. We find that the system is dynamically trapped in the neighborhood of the initial state, and the quantum evolution is related to the local curvature of the chosen minima, i.e., for higher curvature the trapping effect is stronger. Our approach opens a new window in the understanding of driving-induced criticality, in particular, the effective Hamiltonian Eq. (20) con-

tains effective interactions which are absent in equilibrium, in this sense, the effective Hamiltonian can be considered as a quantum simulator. Surprisingly, despite of the close relation between the LMG model and the Dicke model, in contrast to our description of the nonequilibrium QPT in the Dicke model [13], the order of the phase transitions in the LMG model does not change under the effect of driving. In the case of undriven QPTs, the critical behavior is related to nonanaliticities of the ground state. Under the effect of an external driving, however, the system will experience transitions to excited states, even if it is initially prepared in the ground state. In this sense, the global minima as well as the local minima of the LQE landscape play the role of driving-induced states of matter.

Acknowledgments

The authors gratefully acknowledge financial support from the DAAD and DFG Grants BR 1528/7 − 1, 1528/8 − 1, SFB 910, GRK 1558, and SCHA 1646/2 − 1.

[1] S. Sachdev, *Quantum Phase Transitions* (Cambridge University Press, Cambridge, England, 1999); R. Gilmore and D. H. Feng, Nucl. Phys. A **301**, 189 (1978); R. Gilmore, J. Math. Phys. **20**, 891 (1979).

[2] A. Pálffy, J. Evers, and C. H. Keitel, Phys. Rev. C **77**, 044602 (2008) .

[3] A. Altland, V. Gurarie, T. Kriecherbauer, and A. Polkovnikov, Phys. Rev. A **79**, 042703 (2009).

[4] A. Polkovnikov , K. Sengupta , A. Silva , and M. Vengalattore, Rev. Mod. Phys. **83**, 863 (2011).

[5] W. Zurek, U. Dorner, and P. Zoller, Phys. Rev. Lett. **95**, 105701 (2011).

[6] J. Gong, L. Morales-Molina, and P. Hänggi, Phys. Rev. Lett. **103**, 133002 (2009).

[7] C. D. Graf, G. Weick, and E. Mariani, Europhys. Lett. **89**, 40005 (2010).

[8] A. Eckardt, C. Weiss, and M. Holthaus, Phys. Rev. Lett. **95**, 260404 (2005).

[9] L. Goren, E. Mariani, and A. Stern, Phys. Rev. A **75**, 063602 (2007).

[10] H. Lignier, C. Sias, D. Ciampini, Y. Singh, A. Zenesini, O. Morsch, and E. Arimondo, Phys. Rev. Lett. **99**, 220403 (2007).

[11] N. H. Lindner, G. Refael, and V. Galitski, Nat. Phys. **7**, 490 (2011).

[12] J. Inoue, and A. Tanaka, Phys. Rev. Lett. **105**, 017401 (2011).

[13] V. M. Bastidas, C. Emary, B. Regler and T. Brandes, Phys. Rev. Lett. **108**, 043003 (2012).

[14] L. Jiang, T. Kitagawa, J. Alicea, A. R. Akhmerov, D. Pekker, G. Refael, J. I. Cirac, E. Demler, M. D. Lukin, and P. Zoller, Phys. Rev. Lett. **106**, 220402 (2011).

[15] P. Ribeiro, J. Vidal, and R. Mosseri, Phys. Rev. E **78**, 021106 (2008) .

[16] P. Pérez-Fernández, P. Cejnar, J. M. Arias, J. Dukelsky, J. E. García-Ramos and A. Relaño, Phys. Rev. A **83**, 033802 (2011); P. Pérez-Fernández, A. Relaño, J. M. Arias, P. Cejnar, J. Dukelsky and J. E. García-Ramos, Phys. Rev. E **83**, 046208 (2011) .

[17] C. Emary and T. Brandes, Phys. Rev. Lett. **90**, 044101 (2003); Phys. Rev. E **67**, 066203 (2003).

[18] M. Macek and A. Leviatan, Phys. Rev. C **84**, 041302(R) (2011) .

[19] H. Lipkin, N. Meshkov, and A. Glick, Nucl. Phys. **62**, 188 (1965); N. Meshkov, A. Glick, and H. Lipkin, Nucl. Phys. **62**, 199 (1965); A. Glick, H. Lipkin, and N. Meshkov, Nucl. Phys. **62**, 211 (1965) .

[20] J. Ma, X. Wang, C. P. Sun, and F. Nori, Phys. Rep. **509**, 89 (2011) .

[21] J. Ma, X. Wang and C. P. Sun, Phys. Rev. A **80**, 012318 (2009) .

[22] S. Morrison and A. S. Parkins, Phys. Rev. Lett. **100**, 040403 (2008) .

[23] S. Morrison and A. S. Parkins, Phys. Rev. A **77**, 043810 (2008) .

[24] J. Larson, Europhys. Lett. **90**, 54001 (2010) .

[25] P. Solinas, P. Ribeiro, and R. Mosseri, Phys. Rev. A **78**, 052329 (2008) .

[26] T. Caneva, R. Fazio, and G. E. Santoro, Phys. Rev. A **78**, 052329 (2008) .

[27] A. Das, K. Sengupta, D. Sen, and B. K. Chakrabarti, Phys. Rev. B **74**, 144423 (2006) .

[28] C. Hicke and M. I. Dykman, Phys. Rev. B **78**, 024401 (2008) .

[29] S. Chaudhury, A. Smith, B. E. Anderson, S. Ghose and P. S. Jessen, Nature (London) **461**, 768 (2009) .

[30] S. Longhi, Phys. Rev. A **83**, 034102 (2011) .

[31] G. Chen, J. Li, and J. Liang, Phys. Rev. B **76**, 054512 (2007) .

[32] V. I. Arnold, *Mathematical Methods of Classical Mechanics* (Springer-Verlag, New York, 1978) .

[33] J. H. Shirley, Phys. Rev. **138**, B979 (1965) .

[34] T. Dittrich, P. Hänggi, G. Ingold, B. Kramer, G. Schön and W. Zwerger, *Quantum Transport and Dissipation* (Wiley-VCH, Weinheim, 1998) .

[35] M. Grifoni and P. Hänggi, Phys. Rep. **304**, 229 (1998) .

[36] S. Ashhab, J. R. Johansson, A. M. Zagoskin, and F. Nori, Phys. Rev. A **75**, 063414 (2007) .

[37] M. Abramowitz and I. A. Stegun, *Handbook of Mathematical Functions with Formulas, Graphs and Mathematical Tables*, edited by M. Abramowitz and I. A. Stegun (Dover, New York, 1972) .

[38] F. Arecchi, E. Courtens, R. Gilmore, and H. Thomas, Phys. Rev. A **6**, 2211 (1972) .